frontiers | Frontiers in Food Science and Technology

TYPE Original Research
PUBLISHED 08 March 2024
DOI 10.3389/frfst.2024.1361817

OPEN ACCESS

EDITED BY
Dong Uk Ahn,
Iowa State University, United States

REVIEWED BY
Karl Matthews,
Rutgers, The State University of New Jersey, United States
Jingwen Gao,
Rutgers, The State University of New Jersey, United States

*CORRESPONDENCE
Lynne McLandsborough,
lm@foodsci.umass.edu
Maria G. Corradini,
mcorradi@uoguelph.ca

†PRESENT ADDRESS
Victor Ryu, Victor Ryu, USDA, ARS, Eastern Regional Research Center, Wyndmoor, PA, United States

RECEIVED 26 December 2023
ACCEPTED 27 February 2024
PUBLISHED 08 March 2024

CITATION
Ryu V, Ghoshal M, Chuesiang P, Ruiz-Ramirez S, McLandsborough L and Corradini MG (2024), Mechanisms of microbial photoinactivation by curcumin's micellar delivery.
Front. Food. Sci. Technol. 4:1361817.
doi: 10.3389/frfst.2024.1361817

Mechanisms of microbial photoinactivation by curcumin's micellar delivery

Victor Ryu[1†], Mrinalini Ghoshal[2], Piyanan Chuesiang[3], Silvette Ruiz-Ramirez[4], Lynne McLandsborough[1*] and Maria G. Corradini[5*]

[1]Department of Food Science, University of Massachusetts Amherst, Amherst, MA, United States, [2]Department of Microbiology, University of Massachusetts Amherst, Amherst, MA, United States, [3]Department of Food Technology, Faculty of Science, Chulalongkorn University, Bangkok, Thailand, [4]Department of Food Science and Technology, Ohio State University, Columbus, OH, United States, [5]Food Science Department and Arrell Food Institute, University of Guelph, Guelph, ON, Canada

Introduction: Microbial photoinactivation using UV light can be enhanced by the addition of food-grade photosensitizers (PSs), such as curcumin. Micellization of curcumin can improve its stability and antimicrobial activity. The objective of this study was to investigate the potential mechanisms that contribute to the photoinactivation of *Escherichia coli* O157: H7 and *Listeria innocua* by curcumin-loaded surfactant solutions produced with Surfynol 465 (S465) or Tween 80 (T80) below, near, and above their critical micelle concentration (CMC).

Methods: Stock curcumin-surfactant solutions were produced with S465 or T80 (5 mM sodium citrate buffer, pH 3.5). Mixtures of each bacterial suspension (initial inoculum = 6 LogCFU/mL), 1 μM curcumin, and surfactants were irradiated with UV-A light (λ = 365 nm) for 5 min. Microbial recovery after treatments was assessed by monitoring the growth of the treated *E. coli* O157: H7 or *L. innocua* using an oCelloscope™. The growth curves were characterized using a modified logistic model.

Results and Discussion: Both gram-positive and gram-negative bacteria showed less and slower recovery when treated with curcumin-S465 (near or at CMC) than curcumin-T80 solutions after irradiation. FLIM micrographs suggested that curcumin was preferentially localized at the cell membrane when S465 was present, as evidenced by its longer lifetimes in samples treated with curcumin-S465 solutions. Washing after treatment resulted in the removal of loosely bound or unbound S465-curcumin micelles; hence, both *E. coli* O157: H7 and *L. innocua* recovery was faster. This suggested that curcumin partitioning has a significant role in microbial photoinactivation, possibly due to the production of reactive oxygen species (ROS) closer to/within the membrane. The permeability of the membrane of *E. coli* O157: H7, as inferred from the Live/Dead cell assay, increased when S465 was present, suggesting that S465 can also facilitate inactivation by disrupting the membrane and by favoring the localization of curcumin adjacent to the cell membrane. Therefore, a synergistic

antimicrobial effect is observed when curcumin is present alongside S465 at concentrations below or near its CMC due to the disruption of the cell membrane by S465.

KEYWORDS

microbial photoinactivation, curcumin, micelle, photosensitizer, critical micelle concentration, growth kinetics, *Escherichia coli* O157:H7, *Listeria innocua*

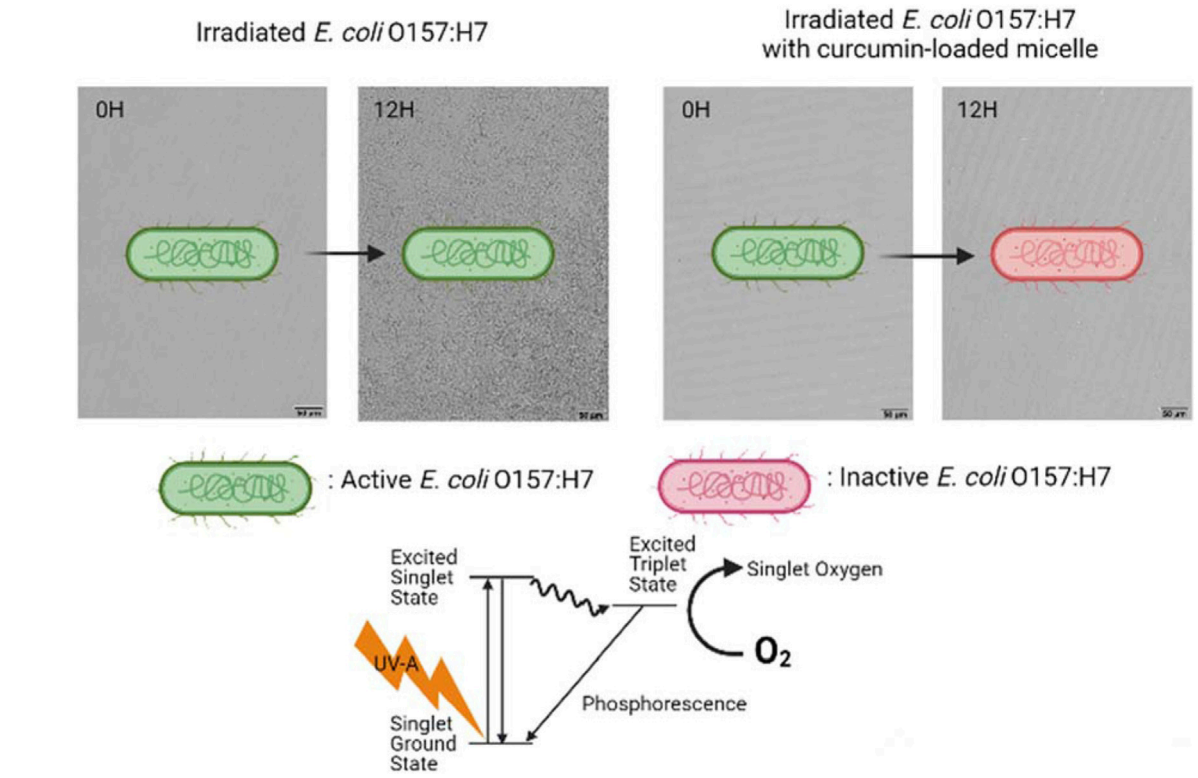

GRAPHICAL ABSTRACT

Highlights

- Microbial photoinactivation efficacy is higher when curcumin-Surfynol 465 micelles are used.
- Surfynol 465 may disrupt the cell's membrane, enhancing inactivation.
- Non-partitioned curcumin may have a significant role in microbial photoinactivation.

1 Introduction

Microbial photodynamic inactivation (PDI) has received considerable attention as a novel strategy for surface sanitation that could potentially replace the currently used methods. PDI uses photosensitizers (PS) in combination with light in the UV or visible range to produce reactive oxygen species (ROS) that lead to microbial inactivation. The use of food-grade PS, such as riboflavin and curcumin, allows extending the application of this technology to food and food preparation surfaces. Another significant advantage of using PDI is that it does not induce resistance in bacteria, unlike other sanitizing agents (Tsai et al., 2009). For instance, multiple studies indicated that certain bacteria could adapt to sanitization using peracetic acid, origanum oil, or quaternary ammonium compounds such as benzalkonium chloride (Langsrud et al., 2003; Romanova et al., 2006; Becerril et al., 2012; Gu et al., 2020). Upon photoexcitation, PSs transfer energy absorbed from the exciting source to acceptor molecules, such as a surrounding substrate or molecular oxygen ($^3O_2$), generating excited singlet oxygen ($^1O_2$) and other ROS (Maisch et al., 2004; Cossu et al., 2021). These ROS react with lipids or proteins in the cellular membrane and at different parts of the microorganism, causing oxidative stress, and eventually leading to the loss of its viability (Cossu et al., 2021). Also, if partitioned deep enough inside the cell, the ROS could react with nucleic acids, DNA and RNA, affecting their functions and producing additional reactive products (Macdonald and Dougherty, 2001; Cossu et al., 2021).

The food-grade PS used in this study is curcumin, a polyphenolic compound found in *Curcuma longa* species. Curcumin has been extensively studied due to its various

beneficial properties as an antibacterial, antifungal, antiviral and anticancer agent (Zorofchian Moghadamtousi et al., 2014). Also, it is used as a colorant in food as it imparts yellow color. This study focuses on the photoactivated antimicrobial effects of curcumin. The PS ability of curcumin has been summarized in several reports (Dahl et al., 1989; Zorofchian Moghadamtousi et al., 2014; de Oliveira et al., 2018; Cossu et al., 2021). Like other PSs used for PDI, such as chlorophyllin, Eosin Y or Rose Bengal, curcumin produces ROS that inactivate bacteria (Cossu et al., 2021).

Although curcumin is an effective PS, its incorporation into aqueous solutions, which are commonly used for washing vegetables, fruits, or food contact surfaces, is deterred by its inherent instability in water (de Oliveira et al., 2018) and limited solubility, i.e., 3.12 mg/L at 25°C (Karaffa, 2013). Curcumin crystallizes at acidic pHs and degrades at basic pHs in the aqueous phase (Tønnesen and Karlsen, 1985). These limitations hinder curcumin's ability to produce ROS such as $^1O_2$ and superoxide (O_2^-) in an aqueous environment. However, previous studies reported that $^1O_2$ production by curcumin was detected once it was encapsulated in micelles, while there was limited detection in the aqueous phase (Chignell et al., 1994). The authors attributed the effective $^1O_2$ production from curcumin enclosed in micelles to a shift in equilibrium towards curcumin's keto form within this sheltered and less protic environment, which has a higher singlet oxygen quantum yield than its enol form (Chignell et al., 1994). In addition, $^1O_2$ is reported to have a lifetime of 10–100 μs in organic solvents while it has a lifetime of 2 μs in aqueous media as the excited-state energy of singlet oxygen dissipates as heat by O-H stretching of the water molecule (Macdonald and Dougherty, 2001). Therefore, an appropriate delivery system should be applied to increase curcumin's stability and performance as an antibacterial agent. Previous studies have shown that curcumin encapsulated in surfactant micelles could be stable for an extended period of time (e.g., over 30 days), which also prolonged its photoactivated antimicrobial activity (Duan et al., 2015; Ryu et al., 2021). Ryu et al. (2021) indicated that the characteristics of the surfactant used to produce curcumin-loaded micelles affect its efficacy. For example, the use of a "Gemini" surfactant such as Surfynol 465 (S465) resulted in synergistic microbial photoinactivation as the surfactant itself had weak bactericidal activity at low pH (Ryu et al., 2021). However, the exact mechanism responsible for this synergism when both curcumin and S465 were present was not investigated. Therefore, we hypothesized that besides curcumin's inherent ability to perform as a PS and produce ROS, the addition of surfactants could potentially enhance (i) light penetration through water, (ii) chemical stability of curcumin, (iii) partitioning of curcumin inside the cell; and (iv) the extent of time required for recovery of the affected microbial population.

In this study, curcumin-surfactant solutions containing different concentrations of Surfynol 465 (S465) or Tween 80 (T80), which are both approved to be used on food contact surfaces, were produced. Photoinactivation efficacy of these curcumin-surfactant solutions was tested against *Escherichia coli* O157:H7 and *Listeria innocua* by observing their recovery after treatment using an oCelloscope™. Also, the contribution of partitioned curcumin to microbial photoinactivation was assessed by washing the cells after incubating them with curcumin or curcumin-surfactant solutions for 1 h. This washing step removes loosely bound and unbound curcumin from the cell membrane, allowing only partitioned curcumin to remain in the studied system. The mechanisms behind the synergistic antimicrobial effect of the S465 micelles loaded with curcumin were assessed using Fluorescence Lifetime Imaging Microscopy (FLIM) and a Live/Dead Cell Assay. The purpose of this approach was to evaluate how the surfactant could enhance curcumin's performance against common foodborne pathogenic bacteria.

2 Materials and methods

2.1 Materials

TCI Chemicals provided the curcumin (C2302-5G, purity > 97%, Montgomeryville, PA, United States). The nonionic surfactants, namely Surfynol 465 (S465) and Tween 80 (T80), were purchased from Shenzhen Vtolo Industrial Co. Ltd (Shenzhen, Guangdong, China) and Sigma-Aldrich (P1754, St Louis, MI, United States), respectively. The 5 mM sodium citrate buffer was prepared using sodium citrate (#775538, Fisher-Scientific, Waltham, MA, United States) and citric acid monohydrate (C7129, Sigma-Aldrich). Pharmco (Brookfield, CT, United States) was the supplier of the absolute ethanol (#111000200).

2.2 Preparation of stock solutions

Curcumin was dissolved in ethanol to prepare a 4 mM curcumin stock solution. The curcumin in ethanol stock solution was titrated at 2.5 mL/min into the surfactant solution (S465 or T80) and stirred with a magnetic stir bar at 125 rpm to obtain a 20 μM curcumin-surfactant stock solution. The surfactant solution was prepared by dissolving S465 or T80 in 5 mM sodium citrate buffer at pH 3.5 for 20 min with agitation. After titration, the stock curcumin micelle solution was stirred for additional 15 min to determine whether there was a high enough surfactant concentration to solubilize the curcumin (Kharat et al., 2017). If the concentration of surfactant were too low, shearing would induce nucleation and crystallization of the curcumin. Filter-sterilization of curcumin micelles was done using a 0.45 μM syringe filter (Cat# 02915-22, Cole-Palmer, Vernon Hills, IL, United States) and stored at 4°C. The concentration of surfactant and curcumin used to produce curcumin-surfactant stock solutions was selected so that 1 μM curcumin and surfactant concentration below, at, or above the critical micelle concentration (CMC) could be obtained after dilution. The curcumin S465 micelles and curcumin T80 micelles average size was about 6.3 and 15 nm respectively as reported by Ryu et al. (2021).

2.3 Encapsulated curcumin after dilution: Stability and photophysical properties

The stability of encapsulated curcumin was determined by diluting the 20 μM curcumin-surfactant stock curcumin to 1: 20 in 5 mM sodium citrate buffer (pH 3.5) and measuring its absorbance at 10 min intervals over 1 h with a UV-visible spectrophotometer (Shimadzu Scientific, Kyoto, Japan). The solutions were placed into 1-cm light path quartz cuvettes

(FireflySci Inc., Staten Island, NY, United States), and their absorbance was measured at 425 nm and 5-nm slit. The fluorescence intensity of the curcumin solution (1 μM) was used to assess the lack of precipitation and stability of the encapsulated curcumin to oxidation. The fluorescence emission spectra of the curcumin and the curcumin-surfactant solutions over time were collected at an excitation wavelength of 365 nm over an emission wavelength range of 375–600 nm using a spectrofluorometer (Fluoromax 4, Horiba Scientific Inc., Edison, NJ, United States). The excitation and emission slits were set at 3 and 4 nm, respectively.

2.4 Preparation and characteristics of the bacterial cultures

E. coli O157:H7 (ATCC-43888, non-toxigenic strain) and *L. innocua* Seelinger (ATCC-51742) were obtained from the American Type Culture Collection (Manassas, VA, United States). A mixture of tryptic soy broth (TSB; Cat# DF0064-07-6, BD Diagnostic Systems, Berkshire, United Kingdom) and 25% v/v glycerol was used to prepare the *E. coli* O157:H7 suspension. The *L. innocua* Seelinger stock solution was prepared in a mixture of tryptic soy broth with 0.01% yeast extract (TSBYE) and 25% v/v glycerol. Both stocks were stored under freezing conditions, i.e., −80°C. A loopful of frozen stock was used to produce the working solutions. After the inoculum was transferred to TSB, it was incubated at 37°C overnight. Then, the working stocks were streak plated onto MacConkey Sorbitol Agar (MCS; Cat# 279100, BD Diagnostic Systems) or Modified Oxford Agar (Cat# 222530, BD Diagnostic Systems) and stored at 4°C for a week.

In order to conduct the photoinactivation assay, a colony of *E. coli* O157:H7 or *L. innocua* was inoculated into TSB or TSBYE, respectively, and incubated at 37°C for 18 h on a 125 rpm shaker. For each experiment, after 18 h, the cultures were diluted, and their optical density at 600 nm (OD600) was measured and adjusted to 0.15 cm^{-1} to verify that the initial culture contained about 9 log CFU/mL. Bacteria were then washed twice with PBS and centrifuged at 2000 *g* for 3 min. The OD600 of the suspensions was determined again after washing to confirm that no significant loss of bacteria took place. The bacterial counts were confirmed by dilution and plating on Tryptic Soy Agar (TSA; Systems Cat# 236920, BD Diagnostic Systems) using the spread plate method. The culture was diluted to obtain an initial inoculum of approximately 6 log CFU/mL.

2.5 Partitioning assay

2.5.1 Sample preparation

Samples were prepared by replacing a volume of the buffer with different volumes of curcumin-surfactant stock solution so that a series of samples with the same curcumin concentration (1 μM) but different surfactant concentrations (below, near, and above the CMC) were attained. The bacteria were then incorporated to reach 6 log CFU/mL. Bacteria were preincubated in the curcumin-surfactant solutions for 1 h in the dark to determine whether the partitioned curcumin had a significant role in their inactivation. They were then washed once with 5 mM sodium citrate buffer (pH 3.5) by centrifugation at 2,000 g for 3 min.

2.5.2 Bacterial photoinactivation

2 mL of each inoculated solution was transferred to 4 wells in sterile 24-well non-treated plates (Celltreat®, #229524, Pepperell, MA, United States). After storing the plates in the dark for 5 min, they were either incubated in the dark or irradiated for 5 min and incubated. The UV irradiation time was selected based on previous efficacy reported with this settings (de Oliveira et al., 2018). The irradiation was performed using an XL-1500 UV-crosslinker (Spectronic Corporate, Westbury, NY, US) equipped with UV-A light (λ = 365 nm). As stated by the Kasha-Vavilov's rule (Jameson, 2014), quantum yield is, in general, not affected by the excitation wavelength. Thus, the irradiation source light was selected near the maximum absorbance wavelength of the curcumin (λ = 424 nm). The 24-well plate was placed inside the irradiation chamber on an elevated platform set up 9 cm away from the light source. The wells xy position was adjusted to ensure exposure of all wells to an irradiance of 5.2–5.4 mW/cm^2. The irradiance and temperature in the wells were corroborated using a UV A/B light meter (#850009, Sper Scientific, Scottsdale, AZ, United States) and a four-channel data logger (#800024, Sper Science), respectively. The independent effects of the UV light, each surfactant type and concentration without curcumin, and non-encapsulated curcumin on microbial inactivation were also tested by setting up adequate controls at the selected pH (i.e., 3.5).

2.6 Bacterial growth after photoinactivation

2.6.1 Monitoring growth using an oCelloscope™

The bacteria's ability to grow and its susceptibility toward photoinactivation was assessed using an oCelloscope™ (BioSense Solution, Farum, Denmark). After photoinactivation, 100 μL of the treated sample was introduced to 200 μL of growth medium (2XTSB) in each well of the 96-well plate. The dilution in TSB stops further photoinactivation by curcumin due to the relatively high pH, i.e., ~7, of the resulting solution (de Oliveira et al., 2018).

The 96-well plate was placed inside the oCelloscope™ at room temperature (~20°C). Ten images were acquired every 1 h for 24 h, the distance for imaging was fixed at 4.9 μm, and the illumination time was 2 m. Growth curves of the bacteria over time were determined based on the background-corrected absorption (BCA) algorithm of the Uniexplorer software (Biosense Solutions, version 10.0). The BCA algorithm utilizes data from the z-stacks and the increase in microbial counts is calculated and reported on a logarithmic (base 10) scale. Also, morphological changes of the bacteria due to the photoinactivation treatment were assessed using best-focus images.

2.6.2 Microbial growth modeling

The BCA value at each time interval (i.e., data recorded hourly for a full day) acquired from oCelloscope™ was used to follow *E. coli* O157:H7 and *Listeria innocua* growth after treatment. The data were characterized using a modified logistic model as described by (Corradini and Peleg, 2005):

$$Y(t) = \frac{a}{1 + \exp(k^*(t - t_c))} - \frac{a}{1 + \exp(k^* t_c)} \quad (1)$$

where $Y(t)$ is the ratio between the momentary and initial BCA values, a provides a measure of the extent of the growth since it corresponds to the maximum value that the growth curve reached, k is the growth rate, and t_c indicates the inflection point of the growth curve, which provides information about the time required by the microorganism to grow. The experimental data were adjusted with Eq. 1 using the nonlinear regression routine available in Mathematica 13.1 (Wolfram Research, Inc. Champaign, IL, United States). The mean squared error was used as a measure of goodness of fit.

2.7 Fluorescence Lifetime Imaging Microscopy (FLIM)

Fluorescence Lifetime Imaging Microscopy (FLIM) was employed to study the characteristics of the local environment around the lumiphore (i.e., curcumin), which can help elucidate the partitioning of this PS into the microbial cells (Colaruotolo et al., 2021). 10 µL of each bacterial culture was placed on a 35 mm poly-D-lysine coated dish (P35GC-1.5-10-C, MatTek Life Sciences, Ashland, MA, United States). Cells were dried for 2 h under air circulation in a biological safety cabinet. Then, they were treated with 5 µM curcumin and S465 or T80 (near CMC). To assess curcumin partitioning, cells were washed with buffer after pre-incubation with 5 µM curcumin and S465 or T80 for 1 h and then dried for 10 min. The fluorescence lifetime measurements were recorded using a Nikon TiE confocal microscope with an A1 Spectral Detector (Nikon Instruments Inc., Melville, NY, United States) equipped with a FLIM/FCS module. Firstly, the traditional scanning confocal capability of the microscope was used to image the fluorescence of curcumin within each sample. Once a suitable field of view was identified and finely focused, the 405 nm pulsed input laser was selected, and the photons emitted were directed to the Becker-Hickl SPC-152/HPM-100–40 dual detector system (Boston Electronics). Curcumin fluorescence lifetime was measured using a 50 MHz pulse frequency. The recorded fluorescence decays were analyzed using the Becker & Hickl SPC Image fitting software. The mean fluorescence lifetime of the 256 × 256 pixel lifetime images was calculated, and the lifetime decay was characterized using a two-exponential model.

2.8 Live/dead cell assay

For irradiated or non-irradiated unwashed *E. coli* O157:H7 with curcumin or surfactants (S465 or T80) a live/dead cell assay was performed to measure the proportion of cells that exhibited a permeable membrane. Equal volumes of Syto 9 (S34854, Thermofisher, Waltham, MA, United States) and propidium iodide (25535-16-14, Sigma-Aldrich) were mixed in a centrifuge tube. 3 µL of the dye mixture was added to 1 mL of the bacterial suspension (7 log CFU/mL). The mixture was then incubated in the dark at room temperature for 15 min 20 µL of the sample was placed on a 35 mm poly-D-lysine coated dish. The fluorescence intensity of the cell-permeable dyes was acquired using a confocal microscope with structured illumination (A1R-SIMe, Nikon Instruments Inc., Melville, NY, United States). Once the appropriate field of view was identified and focused, a 488 nm laser was selected to excite the dyes. Obtained micrographs were analyzed using the NIS-Elements software (Nikon Instruments Inc.) to determine the proportion of cells in the sample with a permeable membrane as indicated by the emission intensity of the propidium iodide.

2.9 Cell injury

The percentage of injured *E. coli* O157:H7 cells in unwashed samples non-irradiated and after irradiation or non-irradiation with curcumin or surfactants (S465 or T80) was determined by comparing the number of colonies on selective (MSC and TSA+2.5%NaCl) and nonselective (TSA) agar. The percentage (%) of injury was calculated using Eq. 2 (Busch and Donnelly, 1992; Espina et al., 2016).

$$Percentage\ of\ injury\ (\%) = \left[1 - \frac{\#\ of\ colonies\ on\ selective\ agar}{\#\ of\ colonies\ on\ nonselective\ agar}\right] * 100 \quad (2)$$

2.10 Data acquisition and analysis

All experiments were performed in triplicate. All statistical analyses were done using $p \leq 0.05$ to represent statistical significance.

3 Results and discussion

3.1 Synergistic microbial photoinactivation by curcumin and surfactant: Potential mechanism

Ryu et al. (2021) identified the synergistic photoinactivation of *E. coli* O157:H7 by curcumin when S465 was present in the 5 mM sodium citrate buffer at pH 3.5. Some of the potential mechanisms responsible for this synergistic effect are i) the increased solubilization of curcumin in the aqueous solution by the presence of the surfactant, which can cause the solution to become more transparent, reducing light scattering and increasing photoexcitation of the curcumin throughout the sample; ii) the improved stability of curcumin in the solution by the addition of the surfactant, prolonging its activity as a PS; and iii) the enhanced partition of curcumin inside the cell by the surfactant physically bringing the curcumin closer to the cell and also causing the cellular membrane to become more permeable. The absorbance of the curcumin-S465 micellar solution was significantly higher than that of curcumin dissolved in ethanol and diluted with buffer, which suggests less turbidity and scatter (Supplementary Figure S1). The surfactant micelles also prevented the nucleation of curcumin, causing an increase in its concentration in the solution and, consequently, its absorbance and fluorescence (Supplementary Figures S2, S3). Curcumin stability after dilution was assessed for 1 h based on the absorbance and the fluorescence emission intensity of diluted curcumin micelle solutions in 5 mM sodium citrate buffer (pH 3.5). The 20 µM stock curcumin micelle solution was diluted to

TABLE 1 Parameters and goodness of fit measures of the growth of *E.coli* O157:H7 after photoinactivation with curcumin-surfactant solutions at different surfactant concentrations, determined using Eq. 1 as a model.

Sample	Surfactant concentration	Parameters[a]			MSE
		a	k	t_c	
		(–)	(h^{-1})	(h)	
Irradiated Control	none	3.54 (3.47–3.61)	0.30 (0.28–0.32)	7.16 (6.90–7.42)	0.0048
Curcumin- S465 (Irradiated)	below CMC	3.49 (3.14–3.83)	0.11 (0.08–014)	28.3 (24.0–32.3)	0.0070
	near CMC	4.12 (3.47–4.77)	0.15 (0.13–0.16)	20.1 (17.8–22.3)	0.0029
	above CMC	3.69 (3.33–4.06)	0.15 (0.14–0.17)	16.5 (15.0–17.9)	0.0031
Curcumin T80 (Irradiated)	below CMC	4.33 (3.78–4.88)	0.15 (0.13–0.17)	17.1 (15.2–19.0)	0.0055
	near CMC	3.91 (3.76–4.07)	0.21 (0.19–0.23)	11.0 (10.5–11.5)	0.0060
	above CMC	3.78 (3.63–3.92)	0.24 (0.22–0.26)	12.4 (12.0–12.9)	0.0051

[a]Confidence intervals (95%) are reported between brackets.

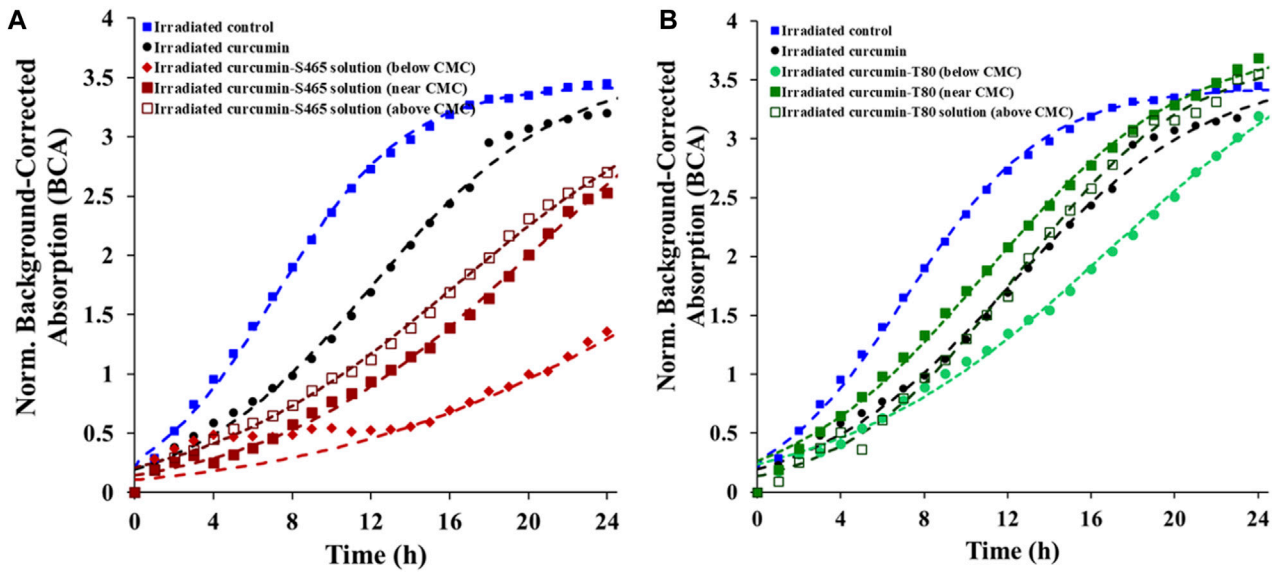

FIGURE 1
Recovery of *E. coli* O157:H7 after treatment with different curcumin surfactant solutions **(A)** S465 and **(B)** T80. Symbols represent experimental data and dashed lines the fit of Eq. 1.

1 μM since this concentration was the one selected for the microbial inactivation assays. The encapsulated curcumin was more stable than the unencapsulated curcumin when either surfactant (S465 or T80) was present (Supplementary Figures S2, S3). Also, more curcumin was present in the solution when a higher concentration of either surfactant was added. It should be noted that the long term stability of the curcumin-surfactant solutions during storage was previously studied and reported, exceeding 30 days at room temperature and under refrigerated conditions (Ryu et al., 2021.) Having established that the presence of surfactants increased the stability and presence of curcumin in the testing solutions, in the consecutive sections, we focused on whether the micelles enhanced the partitioning of curcumin inside the cell.

3.2 Contribution of each of the components of curcumin surfactant solutions to photoinactivation

3.2.1 Surfactant level contributions to cell injury during photoinactivation with curcumin

An oCelloscope™ was used to study cell recovery after photoinactivation using curcumin, surfactants, and UV-A light. The efficacy of the treatments was determined based on the values of growth parameters obtained by characterizing the growth curves with Eq. 1. This model's parameters, *a*, *k* and t_c, provide insights into the extent of growth, growth rate, and time required for effective recovery of the cells and their growth, respectively. Using the parameters in combination rather than

TABLE 2 Parameters and goodness of fit measures of the growth of *E. coli* O157:H7 treated with curcumin-surfactant solutions or their individual components, determined using Eq. 1 as a model.

Sample	Treatment	Irradiated	Parameters[a]			MSE
			a	K	t_c	
			(–)	(h^{-1})	(h)	
Control	Unwashed	NO	3.59 (3.53–3.64)	0.42 (0.39–0.46)	4.72 (4.52–4.93)	0.0058
		YES	3.87 (3.81–3.94)	0.37 (0.34–0.40)	5.24 (5.09–5.41)	0.0015
	Washed	NO	3.90 (3.84–3.96)	0.30 (0.27–0.34)	6.63 (6.28–6.97)	0.0120
		YES	3.64 (3.46–3.89)	0.44 (0.40–0.48)	5.89 (5.80–5.98)	0.0017
Curcumin	Unwashed	NO	3.82 (3.75–3.88)	0.45 (0.41–0.49)	4.29 (4.10–4.50)	0.0078
		YES	3.76 (3.58–3.94)	0.23 (0.20–0.26)	7.69 (7.03–8.36)	0.0184
	Washed	NO	3.32 (3.27–3.37)	0.30 (0.29–0.32)	8.38 (8.18–8.57)	0.0024
		YES	3.95 (0.18–0.21)	0.17 (0.16–0.18)	20.6 (19.5–21.7)	0.0008
S465	Unwashed	NO	3.88 (3.81–3.95)	0.38 (0.35–0.41)	4.94 (4.70–5.20)	0.0085
		YES	3.63 (3.57–3.70)	0.29 (0.27–0.31)	8.86 (8.63–9.09)	0.0035
	Washed	NO	3.46 (3.35–3.58)	0.20 (0.19–0.21)	13.9 (13.5–14.3)	0.0013
		YES	3.89 (3.73–4.05)	0.24 (0.21–0.26)	9.34 (8.80–9.90)	0.0120
Curcumin-S465 micelle (near CMC)	Unwashed	NO	3.79 (3.71–3.86)	0.35 (0.32–0.39)	5.54 (5.26–5.81)	0.0092
		YES	4.67 (4.05–5.26)	0.17 (0.14–0.20)	21.1 (20.0–22.2)	0.0167
	Washed	NO	4.18 (4.02–4.34)	0.20 (0.19–0.22)	11.5 (10.9–12.0)	0.0049
		YES	4.42 (3.81–5.00)	0.16 (0.12–0.19)	12.3 (10.1–14.5)	0.0297
T80	Unwashed	NO	4.30 (4.15–4.45)	0.31 (0.27–0.36)	6.48 (6.00–6.96)	0.0280
		YES	4.02 (3.91–4.11)	0.30 (0.28–0.32)	7.92 (7.64–8.18)	0.0068
	Washed	NO	4.03 (3.90–4.16)	0.27 (0.23–0.30)	6.16 (5.73–6.65)	0.0170
		YES	3.84 (3.75–3.94)	0.28 (0.26–0.31)	7.88 (7.57–8.51)	0.0066
Curcumin-T80 micelle (near CMC)	Unwashed	NO	3.63 (3.52–3.73)	0.32 (0.28–0.36)	6.86 (6.48–7.24)	0.0132
		YES	3.91 (3.76–4.07)	0.21 (0.19–0.23)	11.0 (10.5–11.5)	0.0060
	Washed	NO	3.94 (3.85–4.07)	0.31 (0.27–0.35)	5.72 (5.38–6.15)	0.0156
		YES	4.19 (3.49–4.89)	0.15 (0.14–0.17)	15.7 (14.2–17.2)	0.0076

[a]Confidence intervals (95%) are reported between brackets.

relying in just a single one of them for comparison complements and enhances data interpretation. Although the maximum growth (a) was similar to the control for all the surfactant levels and types, the growth rate (k) was slower, and the time for effective recovery (t_c) was longer when both curcumin and surfactants were present (Table 1; Figure 1). However, all samples treated with solutions produced with T80 as a surfactant had a faster recovery rate (k) than when S465 was used (Table 1; Figure 1). Similarly, the time required for effective recovery (t_c) was longer for the S465 solutions. By comparing a, k and t_c, which for S465 indicated that growth reach a similar level but at a slower pace and after a much longer time, it can be inferred that a more detrimental and permanent effect is observed when S465 rather than T80 was used. It should also be noted that the surfactant concentration also affected the recovery rate, k, (below CMC < near CMC < above CMC) and the time required for recovery, t_c, (below CMC > near CMC > above CMC), which would correlate to the level of damage exerted by each curcumin–surfactant solution. The solubilization of curcumin in surfactant micelles could bring the curcumin and the cells closer together in the aqueous phase. This is important as all ROS are unstable, and if generated too far from the target, they would be quenched before triggering reactions necessary for the photoinactivation of cells. Despite the advantageous effects of delivering the curcumin using surfactant micelles, the micelles could also prevent curcumin from participating in photosensitization of the cell if it is buried deep within the micelle, limiting ROS from reaching the cell (Hammer et al., 1999). Therefore, cells treated with curcumin-surfactant solutions at surfactant concentrations above the CMC were the least effective and showed the fastest recovery rate (k) among the three solutions.

10.3389/frfst.2024.1361817

TABLE 3 Parameters and goodness of fit measures of the growth of *L innocua* treated with curcumin-surfactant solutions or their individual components, determined using Eq. 1 as a model.

Sample	Treatment	Irradiated	Parameters[a]			MSE
			a	K	t_c	
			(–)	(h^{-1})	(h)	
Control	Unwashed	NO	3.56 (3.47–3.64)	0.33 (0.31–0.35)	11.0 (10.8–11.3)	0.0047
		YES	3.58 (3.54–3.61)	0.32 (0.30–0.33)	11.2 (11.0–11.4)	0.0032
	Washed	NO	3.84 (3.33–4.38)	0.33 (0.23–0.42)	14.5 (13.3–16.0)	0.0789
		YES	3.23 (3.04–3.42)	0.24 (0.20–0.27)	11.4 (10.7–12.1)	0.0010
Curcumin	Unwashed	NO	3.76 (3.50–4.00)	0.35 (0.28–0.42)	13.3 (12.7–14.1)	0.0034
		YES	2.03 (1.82–2.24)	0.09 (0.09–0.10)	24.7 (22.2–27.3)	0.0011
	Washed	NO	3.34 (2.97–3.70)	0.34 (0.25–0.42)	14.2 (13.2–15.3)	0.0048
		YES	2.42 (2.07–2.77)	0.15 (0.14–0.16)	21.2 (19.2–23.2)	0.0006
S465	Unwashed	NO	1.96 (1.85–2.06)	0.55 (0.40–0.70)	19.0 (18.4–19.6)	0.0230
		YES	1.02 (0.94–1.09)	0.74 (0.42–1.06)	22.7 (22.1–23.4)	0.0110
	Washed	NO	1.84 (1.58–2.09)	0.14 (0.13–0.16)	17.6 (15.4–19.7)	0.0010
		YES	0.33 (0.31–0.35)	1.30 (1.26–1.34)	2.15 (1.45–2.85)	0.0011
Curcumin-S465 micelle (near CMC)	Unwashed	NO	1.23 (1.14–1.36)	0.36 (0.24–0.46)	18.9 (17.9–20.1)	0.0120
		YES	0.86 (0.84–0.89)	0.12 (0.11–0.13)	5.30 (4.01–6.70)	0.0001
	Washed	NO	1.23 (1.15–1.31)	0.17 (0.15–0.20)	5.41 (4.47–6.35)	0.0012
		YES	0.53 (0.43–0.63)	2.62 (2.42–2.82)	0.78 (0.08–1.50)	0.0023
T80	Unwashed	NO	3.93 (3.64–4.22)	0.29 (0.24–0.34)	12.8 (12.0–13.6)	0.0300
		YES	3.56 (3.25–3.87)	0.27 (0.22–0.32)	14.0 (13.1–15.0)	0.0021
	Washed	NO	3.73 (3.39–4.08)	0.34 (0.26–0.42)	14.0 (13.1–14.9)	0.0444
		YES	5.54 (5.04–6.04)	0.15 (0.14–0.16)	26.5 (25.1–27.9)	0.0070
Curcumin-T80 micelle (near CMC)	Unwashed	NO	3.72 (3.59–3.86)	0.28 (0.25–0.31)	10.8 (648–7.24)	0.0132
		YES	1.59 (1.29–1.89)	0.30 (0.23–0.37)	20.4 (17.8–23.4)	0.0035
	Washed	NO	3.64 (3.26–4.02)	0.24 (0.19–0.28)	13.3 (12.1–14.5)	0.0270
		YES	2.19 (1.23–3.14)	0.11 (0.10–0.12)	28.7 (21.7–35.7)	0.0006

[a]Confidence intervals (95%) are reported between brackets.

All the results were consistent with the previous study that evaluated the microbial photoinactivation efficacy of curcumin-surfactant solutions using the most probable number (Ryu et al., 2021).

It was also noticed that all treated cells had similar initial BCA values (t = 0 min) (Supplementary Figure S4). The BCA value correlates to the number of cells in the evaluated solution at a given time. The lysis of cells leads to a decrease in the initial BCA value, as seen in a study that used antibiotics (McLaughlin and Sue, 2018). Since the initial BCA values are similar while the number of viable cells decreased, it shows that the microbial photoinactivation using curcumin or curcumin-surfactant solutions can be considered non-lytic (Supplementary Figure S4). The cause of superior antimicrobial efficiency when S465 was employed was further investigated by observing the contribution of individual components of the solution to microbial photoinactivation. See Section 3.6 for a discussion on the proposed mechanisms of action.

3.2.2 Contribution of other components of curcumin surfactant solutions to photoinactivation

In this section, the contribution of each of the components of the curcumin-surfactant solutions to microbial inactivation on non-irradiated and irradiated samples was investigated by observing the recovery of the treated cells over time using the oCelloscope™. Curcumin-surfactant solutions at surfactant concentration near CMC were used for evaluation. This condition was chosen as the encapsulated curcumin in the surfactant solution at a concentration near CMC had higher solubility and better stability while maintaining its antimicrobial activity than those below or above CMC (Figure 1, Supplementary Figure S2) (Ryu et al., 2021). The extent (*a*), rate (*k*),

TABLE 4 Plate count reductions, percentage of *E. coli* O157:H7 cells with permeable membrane, and injured cells after different treatments.

Sample	Treatment	Log reduction	*E. coli* O157:H7 with permeable membrane (%)	% Injured cells
				TSA+2.5%NaCl
Control	Non-Irradiated	0.00 ± 0.0	0.0 ± 0.0	3.78 ± 5.0
	Irradiated	0.01 ± 0.1	9.0 ± 1.0	11.3 ± 7.0
1 μM curcumin	Non-Irradiated	0.01 ± 0.1	10.0 ± 6.0	12.9 ± 9.0
	Irradiated	3.40 ± 0.2	65 ± 12	74.7 ± 16
S465	Non-Irradiated	0.05 ± 0.1	79 ± 7.0	6.48 ± 9.0
	Irradiated	3.00 ± 0.1	75 ± 9.0	87.4 ± 4.0
Curcumin in S465 micelles	Non-Irradiated	0.09 ± 0.2	10 ± 5.0	−4.35 ± 3.0
	Irradiated	4.20 ± 0.3	73 ± 12	52.0 ± 10
T80	Non-Irradiated	−0.02 ± 0.1	0.4 ± 0.3	4.06 ± 4.0
	Irradiated	0.10 ± 0.02	5.9 ± 3.0	15.4 ± 2.0
Curcumin in T80 micelles	Non-Irradiated	0.05 ± 0.1	0.2 ± 0.1	0.76 ± 8.0
	Irradiated	3.20 ± 0.2	35.0 ± 5.0	64.4 ± 7.0

and recovery time (t_c) of the non-irradiated samples were similar to the *E. coli* O157:H7 control for all the tested systems (Table 2). Interestingly, non-irradiated *L. innocua* inoculated samples exposed to S465, with or without curcumin, exhibited a lower growth level (a), slower rate (k) and required more time for recovery (t_c), which attested to the contribution of this surfactant to microbial inactivation (Table 3, Supplementary Figure S5) since the population grew slower and to a lesser extent. The recovery of irradiated *E. coli* O157:H7 and *L. innocua* treated with S465 alone or combined with curcumin was slower than that of the systems containing T80 (Tables 2, 3). Neither surfactant exhibits an absorbance peak at 365 nm, the wavelength used to excite curcumin in this study, as shown in Supplementary Figure S1. Therefore, no photosensitization effect could be attributed to either surfactant. Their contributions to inactivation and slow recovery are possibly due to the increase in permeability or perturbation of the cell membrane when surfactants are present, allowing increased interaction between the ROS produced by irradiation with UV-A light and bacterial DNA or proteins on cellular membrane (De La Maza et al., 1992; Yang et al., 2019). S465 is a Gemini-shaped surfactant with two hydrophobic tails, two ethoxylated hydrophilic groups, and a hydrophilic-lipophilic balance (HLB) value of 13 (Gaysinsky, 2004). T80 is a more linear-shaped surfactant with a hydrophilic polyoxyethylene head group, a hydrophobic tail with a kink, and an HLB value of 15 (Komaiko and McClements, 2016). The Gemini structure of S465 may have benefits over monomeric ones in interacting with the cell. According to Sharma et al. (2005), synthesized dimeric alkanolamine-based cationic "Gemini" surfactants were more efficient in inhibiting *E. coli* and *Bacillus subtilis* growth than their monomeric counterparts. They attributed this effect to the increased interaction between the cell and the surfactant due to a higher number of polar heads and hydrophobic tail groups in this kind of surfactant (Sharma et al., 2005). Another study evaluated the antimicrobial activity of Surfynol 485W (S485W) micelles. In comparison to S465, S485W has a molecular structure with additional hydrophilic ethylene oxide groups (30 instead of 10 mol) and a higher HLB value (18 instead of 13) (Gaysinsky et al., 2005). The differences in potential interactions with other compounds and structures, e.g., membranes, between the two Gemini surfactants might explain the weak antimicrobial activity of S485W against *E. coli* O157:H7 and *Listeria monocytogenes* at pH 5, as previously reported by Gaysinsky et al. (2005). In the current study, S465 also showed higher but still relatively weak antimicrobial activity against *E. coli* O157:H7 at pH 3.5, which was enhanced in irradiated samples. We could conclude that cells were more vulnerable to S465 than T80 due to differences in the molecular structure of surfactants as they dominate their interfacial properties, stability, and micellization.

L. innocua was more vulnerable to photoinactivation than *E. coli* O157:H7. In all the irradiated samples, the extent (a), rate (k), and time required for recovery (t_c) were lower, slower, and generally took longer, respectively (Tables 2, 3). As mentioned before, *L. innocua* was especially vulnerable to S465 even without irradiation. A higher susceptibility of gram-positive bacteria to photosensitizers has been reported due to the difference in cell membrane structure between gram-positive and gram-negative bacteria (Ryu et al., 2021). The outermost layer of gram-positive bacteria is constituted of thick peptidoglycans. In contrast, gram-negative bacteria have an outer lipid layer (lipopolysaccharides and lipoproteins) on top of their inner wall (two to three layers of peptidoglycans). The thick peptidoglycan layer is porous. Hence, it allows small molecules to enter, while the outer lipid layer in gram-negative bacteria better regulates the permeability of small molecules to enter. Therefore, more curcumin may have been able to partition deeper into the cellular membrane of *L. innocua* (gram-positive) than *E. coli* O157:H7 (gram-negative).

3.3 Cell injury

The percentage of injured cells was evaluated by comparing the growth of the treated bacteria in TSA alone and in TSA with sodium chloride at 2.5%. Since *L. innocua* numbers after being

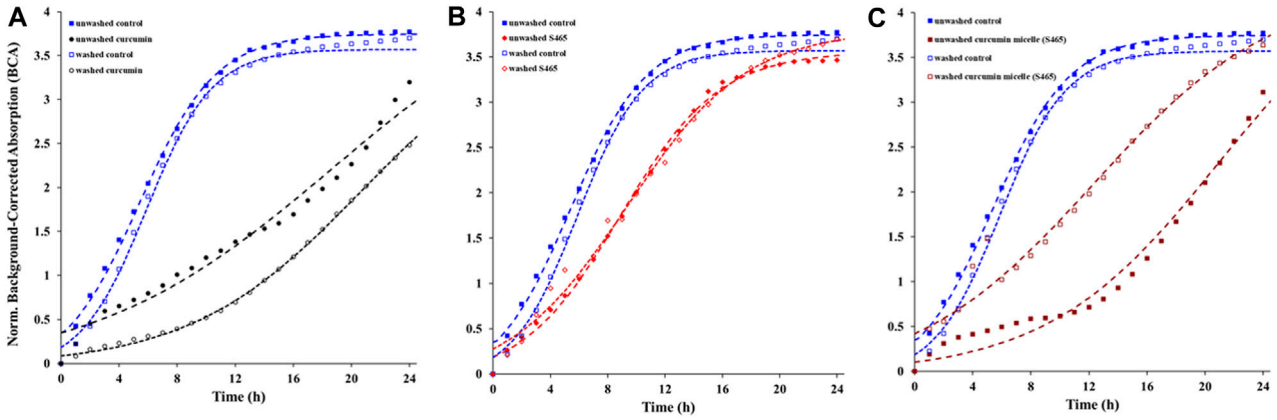

FIGURE 2
Recovery of washed and unwashed *E. coli* O157:H7 irradiated and treated with **(A)** curcumin, **(B)** S465, **(C)** curcumin S465 solution. Symbols represent experimental data and dashed lines the fit of Eq. 1.

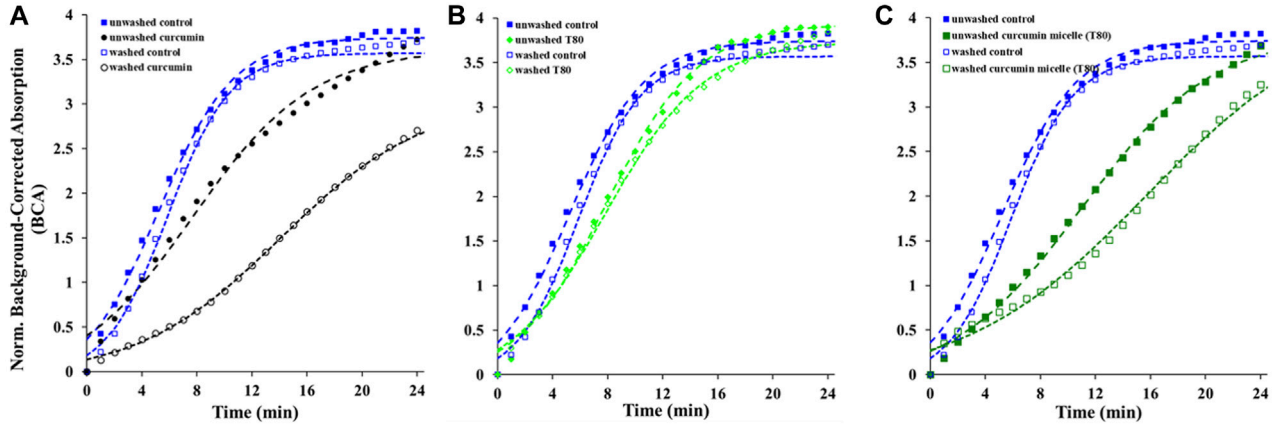

FIGURE 3
Recovery of washed and unwashed *E. coli* O157:H7 irradiated and treated with **(A)** curcumin, **(B)** T80, **(C)** curcumin T80 solution. Symbols represent experimental data and dashed lines the fit of Eq. 1.

treated with curcumin-S465 solutions and irradiated were below the limit of detection of the method, only *E. coli* O157:H7 was used for this part of the study. Cell injury was assessed to determine how many cells were still viable after treatments since the growth curves from oCelloscope™ could not distinguish whether the overall growth resulted from the contribution of one or many cells. The addition of curcumin increased the permeability of the cell membrane after irradiation, suggesting that the generated ROS reacted with components in the cellular membrane (Table 4). The irradiated cells treated with the solutions, including either curcumin or S465, had a higher percentage of injured cells than T80. However, it should be noted that cells treated with the curcumin-S465 micellar solution had the highest number of inactivated cells, indicated by the highest log reduction. Therefore, the reported overall number of cells that could be injured was affected by the overall higher lethality in the curcumin-S465 micellar solution. In general, the results were consistent with the rate and length of time for recovery of *E. coli* O157:H7 obtained using the oCelloscope™. Hence, the oCelloscope™ results correlate well with the proportion of cells that could have been inactivated or injured.

3.4 Contribution of partitioned curcumin to photoinactivation

The contribution of the partitioned curcumin to microbial photoinactivation was studied by preincubating cells with curcumin-surfactant solutions for 1 h in the dark and washing the suspension with buffer before irradiation. During the washing step, the unbound or loosely-bound curcumin (or curcumin-surfactant) to the cell membrane was eliminated. The recovery of the washed cells was observed using the oCelloscope™. For all samples without curcumin, their growth parameters did not differ extensively after washing from those of the unwashed samples. In the case of the samples containing non-encapsulated curcumin or curcumin-T80

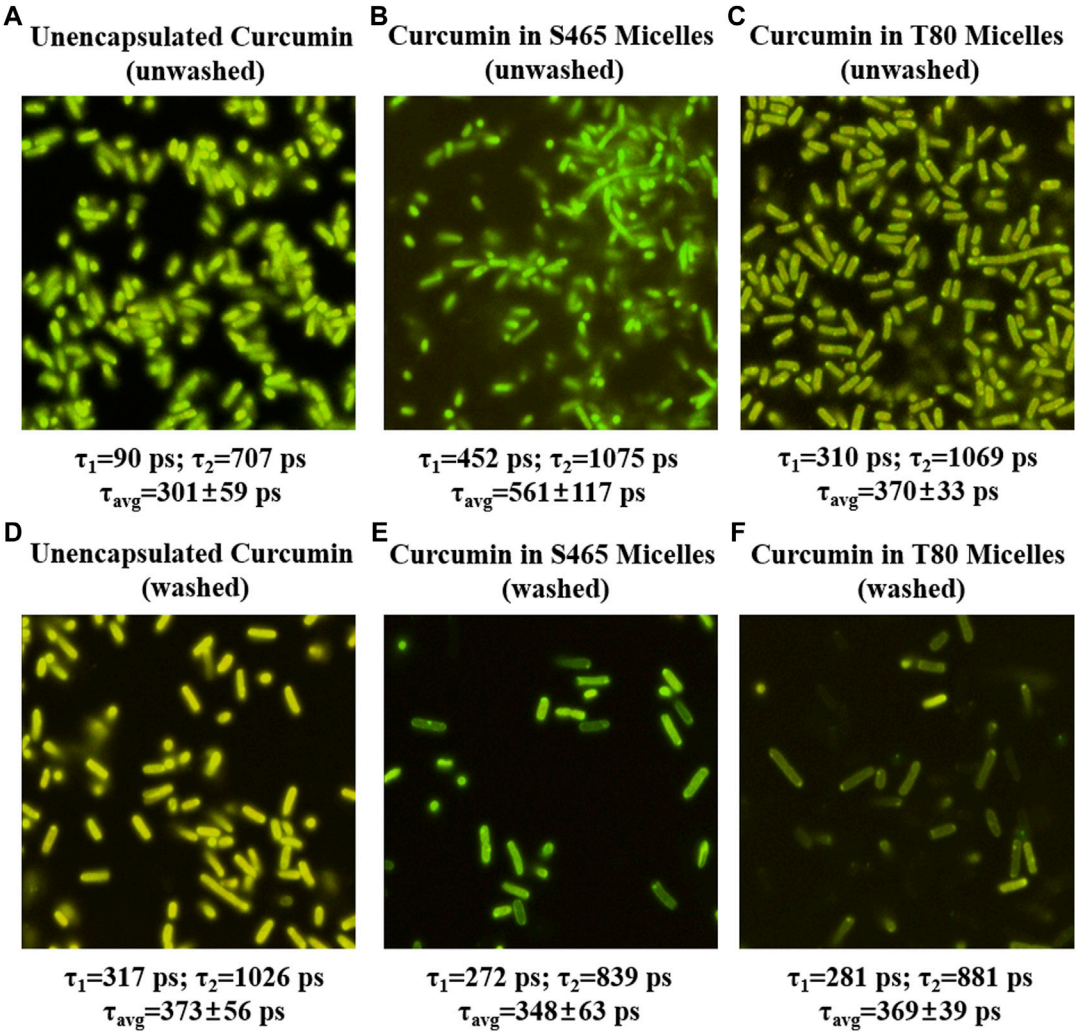

FIGURE 4
FLIM micrographs of *E. coli* O157: H7 immediately after treatment (0 h, unwashed) with unencapsulated curcumin **(A)**, curcumin-S465 micelles **(B)** and curcumin-T80 micelles **(C)** and after applying treatment, waiting for 1 hour and washing (**(D–F)**, respectively). The corresponding short and long components of the exponential fit of the lifetimes are listed below each image along their average lifetime.

micellar solutions, the comparison of the parameters of the model (Eq. 1) revealed that the rate of recovery was slower, and the time required for recovery was longer for washed cells compared to that of the unwashed ones (Figures 2, 3; Supplementary Figures S5, S6; Tables 2, 3). A possible explanation for increased effectiveness in PDI in the washed samples treated with curcumin is that light absorption could have been higher due to the removal of extracellular curcumin, reducing scattering and increasing ROS generation and reactions with the cell. It should be noted that the curcumin average lifetime in the non-encapsulated and T80-curcumin samples before and after washing is very similar, which supports that some curcumin might have been internalized and cannot be removed by washing, remaining effective during growth (Figure 4). Conversely, in the case of the samples treated with curcumin-S465 micellar solutions, the recovery after washing is faster. This may have been due to the removal of curcumin encapsulated in surfactant micelles that could have been adjacent to the cell and the consequent interruption of its inactivating effect on the cells. This also aligns with a reduction of the curcumin average lifetime in the washed samples due to the removal of curcumin latched to the membrane, as will be further discussed in the next section. Therefore, the unbound curcumin or loosely-bound curcumin adjacent to the cell could have a significant role in the photoinactivation of bacteria. Again, the presence of surfactant increases the curcumin concentration in the proximity of the cells, which could be photoexcited and produce ROS. Dahl et al. (1989) evaluated whether the penetration of cell membrane by unencapsulated curcumin was necessary for microbial inactivation by irradiating *Salmonella* Typhimurium, *E. coli, Sarcina lutea,* and *Staphylococcus aureus* preincubated with curcumin for 60 or 90 min and subsequently washed. Their results indicate that washing removed unbound or loosely-bound curcumin and reduced inactivation efficacy, which is consistent with the results of the curcumin-S465 micellar solutions herein (Dahl et al., 1989).

Removing the unbound or loosely-bound portion of curcumin could also have prevented depletion of oxygen near the cells as photoinactivation depends on the presence of oxygen, which might

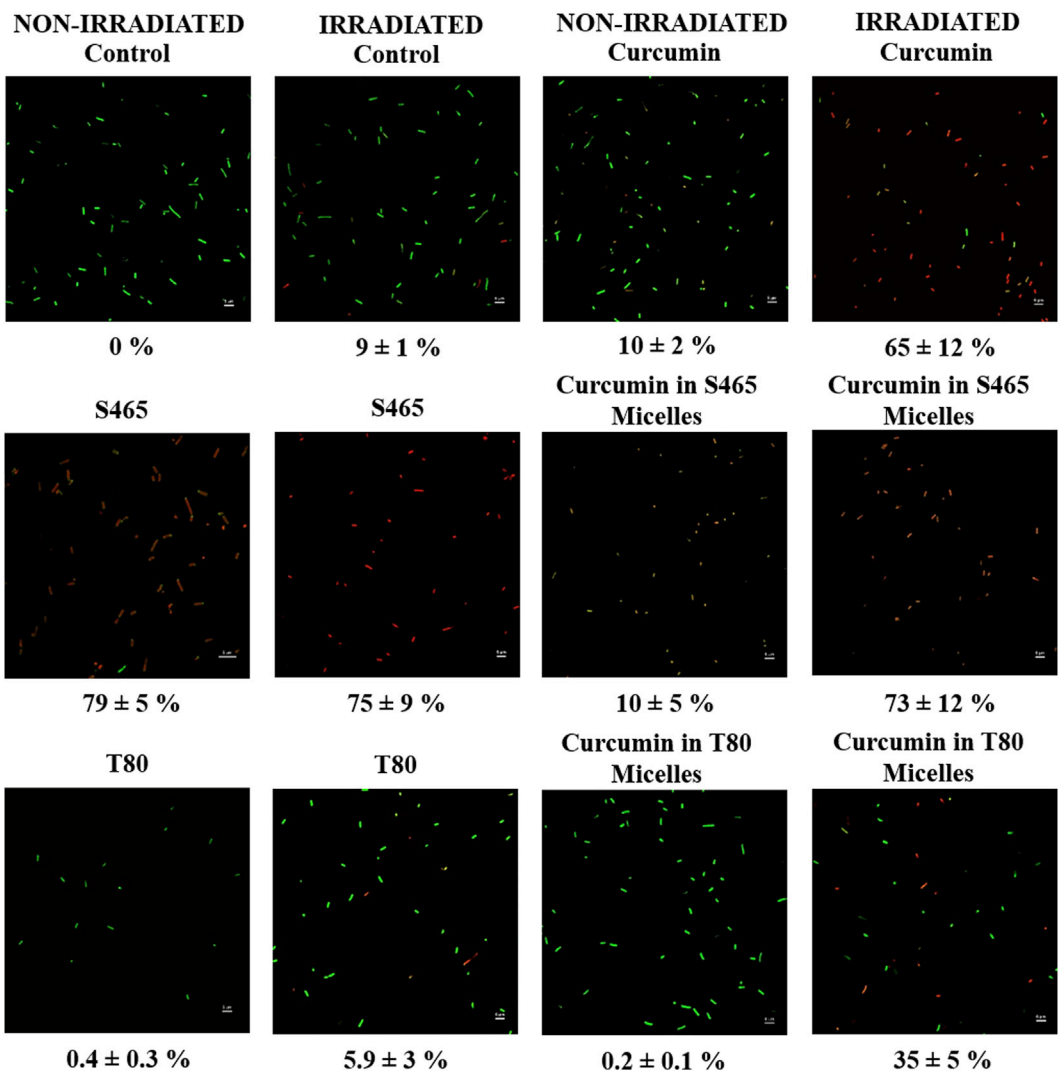

FIGURE 5
Micrographs of non-irradiated and irradiated *E. coli* O157: H7 treated with unencapsulated curcumin, S465, curcumin-S465 micelles, T80, or curcumin-T80 micelles and stained with Syto9 and propidium iodide. Below each image, the percentage of cells with permeable membranes (red) is listed.

have also contributed to the slower recovery in the non-encapsulated curcumin and the T80-curcumin samples. In the samples treated with curcumin-S465 micellar solution, the potential differential location of the PS (i.e., predominately in the membrane surface rather than internalized) resulted in a faster recovery in washed samples despite less oxygen depletion. The effect of S465 on the partitioning of curcumin in cell membranes was further investigated using FLIM and Live/Dead cell assay in the consecutive sections.

3.5 Fluorescence lifetime imaging microscopy (FLIM)

FLIM was used to gain insights into the location and state of the PS, i.e., curcumin, in washed and unwashed cells. Curcumin in the extracellular aqueous phase will exhibit a shorter lifetime than curcumin bound to or enclosed in cellular structures due to the restriction in movement of the fluorophore imposed by the surrounding structures. Curcumin in the extracellular aqueous phase is expected to have a shorter fluorescence lifetime as the excited curcumin would preferentially return to the ground state through non-radiative decay. Although the lifetimes of both curcumin bound to cellular structures and inside the cell are expected to be longer than those of curcumin in the extracellular matrix, a higher degree of restriction imposed by cellular structures in the former will determine longer lifetimes for curcumin molecules bound to, for example, the cell membrane. Hence, the longer fluorescence lifetimes suggest a different environment around curcumin than free ones in extracellular fluid, i.e., bound or inside the cell. For unwashed *E. coli* O157:H7 and *L. innocua* treated with curcumin or curcumin-surfactant solutions (near CMC), the averaged fluorescence lifetimes decreased in the following order: S465 > T80 >and unencapsulated curcumin, respectively (Figure 5; Supplementary Figure S7). Fluorescence

lifetimes can be correlated to photoinactivation efficiency since longer residences in the excited state could result in a more sustained production of ROS (Turro, Ramamurthy and Scaiano, 2017). Therefore, the order of the length of fluorescence lifetime was consistent with the growth parameters reported in Tables 2, 3, e.g., less and slower growth for samples treated with curcumin-S465 micelles. The reason curcumin-S465 solutions had the longest fluorescence lifetime may be due to the different local environment around curcumin when combined with the different types of surfactants. Chignell et al. (1994) reported that the $^1O_2$ phosphorescence generated by curcumin encapsulated in Triton X-100 micelle could be detectable, while there was no $^1O_2$ phosphorescence emission in samples where curcumin was encapsulated in sodium dodecyl sulfate (SDS) micelles (Chignell et al., 1994). The authors attributed this effect to curcumin being located at the hydrophobic region of Triton X-100 micelle, as curcumin in Triton X-100 exhibited similar photophysical properties as when dissolved in toluene (Chignell et al., 1994). Therefore, the free volume and packing around curcumin could have been different when encapsulated in S465 or T80 since these surfactants have different structures and micellization properties, leading to differences in the local environment around curcumin. Also, they point out that $^1O_2$ production by curcumin depends on the hydrophobicity and hydrophilicity of the environment as it influences the predominant tautomer formed (enol vs. keto) which affects its ability to generate $^1O_2$ (Chignell et al., 1994).

After removing extracellular and loosely-bound curcumin by washing, curcumin remained active to a lesser degree, indicating that the remaining curcumin may have partitioned inside both gram-positive and gram-negative cells. The fluorescence lifetimes of curcumin in washed *E. coli* O157:H7 treated with unencapsulated curcumin were longer than those treated with curcumin-surfactant solutions produced with both T80 and S465 (Figure 4). However, the differences between fluorescence lifetimes of curcumin in *L. innocua* were not significantly different between the treatments (Supplementary Figure S7). This may have been due to the different degrees of restriction on partitioned curcumin imposed by different membrane structures in gram-positive and gram-negative cells. Also, the order of length of fluorescence lifetime of curcumin changed when cells were washed compared to when they were not (Unencapsulated > T80 = S465 vs. S465 > T80>Unencapsulated). Fluorescence lifetime is independent of the fluorophore concentration. This helps us assume that the observed changes in the photophysical properties are not related to an increase/decrease in curcumin concentration during the washing step. Demidova and Habmlin (2005) reported that the type of PS affects its ability to bond with cell membranes and could have different efficacy toward gram-positive and gram-negative bacteria (Lauro et al., 2002; Demidova and Hamblin, 2005). They show that PS-poly-L-lysine chlorin conjugates are still effective even after preincubation for 20 min and washing on both gram-positive and gram-negative cells. Other PS, such as Rose Bengal and toluidine blue, were rendered ineffective or became less effective after washing, respectively (Demidova and Hamblin, 2005). Therefore, surfactants or washing may have promoted the loss of unbound or loosely-bound curcumin adjacent to the cell, leading to inefficient photoinactivation when washed. We could conclude that loosely bound and unbound encapsulated curcumin adjacent to the cell may play a significant role when used for photoinactivation in the case of curcumin.

3.6 Live/dead cell assay

A Live/Dead cell assay was used to determine whether the cellular membrane became permeable or not after each treatment. Since *L. innocua* was vulnerable to S465 even without irradiation, only unwashed *E. coli* O157:H7 was used to observe the effect of different treatments on its membrane. *E. coli* O157:H7 treated with S465 had the highest number of cells with increased membrane permeability, whether the samples were irradiated or not (Figure 5; Table 4). Conversely, *E. coli* O157:H7 treated with T80 had the lowest number of cells with a permeable membrane. Data on the recovery of cells after treatment from the oCelloscope™ indicated that photoinactivation of cells by curcumin was non-lytic. Also, it showed that increased membrane permeability did not necessarily result in cell inactivation. If this was the case, the samples treated with S465 solutions should have also shown higher inactivation even before irradiation, according to the results in Tables 2, 3. As expected, the irradiated cells treated with curcumin had more permeable membranes than the non-irradiated ones (Figure 5). This indicates that ROS produced by curcumin could also disrupt the cell membrane, causing it to be permeable. Interestingly, when a curcumin-S465 solution was used to treat the cells, the number of cells with permeable membranes was less before irradiation than when cells were treated with curcumin or S465 alone. However, once irradiated, the number of cells with permeable membranes increased to a similar level as cells treated with S465 alone. This could indicate that when cells were exposed to a curcumin-S465 micellar solution, most of the curcumin or S465 did not react with the membrane as they formed the micelle. However, once irradiated, the micelles adjacent to the cell may have disrupted the cell membrane by producing ROS within a distance short enough for $^1O_2$, the most stable form of ROS, to be effective. $^1O_2$ half-life is typically lower than 3.5 microseconds, allowing it to diffuse distances shorter than 100 nm before being inactivated (Macdonald and Dougherty, 2001; Schweitzer and Schmidt, 2003; Dysart and Patterson, 2005). In addition, it may explain why the fluorescence lifetimes were longer for cells treated with the curcumin surfactant solution produced with S465, as the curcumin could have localized differently in the cell membrane that became more permeable. Cells treated with curcumin-T80 solution had the fewest cells with permeable membranes compared to other treatments. However, the results of a previous study and the data in Figure 5 indicate that the curcumin-T80 solution had similar antimicrobial efficacy to curcumin alone (Ryu et al., 2021). This suggests that cell membrane permeation may contribute but may not be necessary to inactivate the cells. Past studies also suggest that T80 has no inhibitory effect but could be used as a carbon source by microorganisms (Inouye et al., 2001; Ryu et al., 2018). Therefore, the reason curcumin-S465 solutions were effective against microorganisms may have been due to S465 being able to disrupt the membrane of the cell and facilitate the differential partition of the PS.

4 Conclusion

In this study, the potential inactivation mechanisms of curcumin surfactant solutions have been investigated. A previous study

indicated that curcumin-S465 micellar solutions with surfactant concentration near CMC had a synergistic photoactivated antimicrobial activity against *E. coli* O157:H7. Initially, we assumed that this was due to the presence of surfactant, which could: i) allow more light to penetrate through the solution due to increased solubilization of curcumin in the aqueous phase; ii) prevent nucleation of curcumin; iii) enhance the partitioning of curcumin inside the cell. Among these assumptions, an increase in the partitioning of curcumin inside the cell was thought to be the reason for more effective inactivation by these systems. The fluorescence lifetime of unwashed and washed cells treated with curcumin or curcumin surfactant solutions indicated that loosely-bound and unbound curcumin on the cell membrane might contribute to bacterial inactivation and that the location of the PS, highly determined by the use of different surfactants, plays an important role in the treatment's efficacy. From the Live/Dead cell assay, we could observe that S465 could increase the permeability of the cell membrane, which could affect the length of fluorescence lifetime of curcumin within the damaged membrane. Therefore, we could infer that S465 allowed for a differential location of the PS adjacent to the cell in ways that facilitated ROS interaction with the cellular components while also damaging the membrane of microorganisms. Although insights into the mechanism of photoinactivation by curcumin could promote developing systems that could enhance the performance of other food-grade PS, additional testing is required to evaluate the performance of this approach in situations prevalent in the industry, e.g., biofilms and actual equipment and food surfaces.

Data availability statement

The original contributions presented in the study are included in the article/Supplementary Material, further inquiries can be directed to the corresponding authors.

Author contributions

VR: Data curation, Formal Analysis, Investigation, Methodology, Validation, Visualization, Writing–original draft, Writing–review and editing. MG: Data curation, Formal Analysis, Investigation, Writing–review and editing. PC: Formal Analysis, Investigation, Writing–review and editing. SR-R: Data curation, Formal Analysis, Investigation, Writing–review and editing. LM: Conceptualization, Data curation, Funding acquisition, Methodology, Project administration, Resources, Supervision, Writing–review and editing. MC: Conceptualization, Data curation, Funding acquisition, Methodology, Project administration, Software, Supervision, Visualization, Writing–original draft, Writing–review and editing.

Funding

The author(s) declare that financial support was received for the research, authorship, and/or publication of this article. This work was supported by the United States Department of Agriculture [USDA NIFA National Needs, TESA (Code F)], the University of Massachusetts Agricultural Experimental Station, the Department of Food Science (MAS00493), and the National Science Foundation Grant ACI-1548562. MC acknowledges the support of the NSERC Discovery Grant program and John E. Evans Leaders Fund (Canada Foundation for Innovation-CFI).

Acknowledgments

The authors thank Dr. James Chambers for assistance with data collection from FLIM microscopy performed in the Light Microscopy Facility and Nikon Center of Excellence at the Institute for Applied Life Science, University of Massachusetts Amherst (RRID: SCR_012248). The contents are solely the authors' responsibility and do not necessarily represent the official views of the SDA, NIFA, NNF, NSF, or NSERC.

Conflict of interest

The authors declare that the research was conducted in the absence of any commercial or financial relationships that could be construed as a potential conflict of interest.

The author(s) declared that they were an editorial board member of Frontiers, at the time of submission. This had no impact on the peer review process and the final decision.

Publisher's note

Supplementary material

The Supplementary Material for this article can be found online at: https://www.frontiersin.org/articles/10.3389/frfst.2024.1361817/full#supplementary-material

References

Becerril, R., Nerín, C., and Gómez-Lus, R. (2012). Evaluation of bacterial resistance to essential oils and antibiotics after exposure to oregano and cinnamon essential oils. *Foodborne pathogens Dis.* 9 (8), 699–705. doi:10.1089/fpd.2011.1097

Busch, S. V., and Donnelly, C. W. (1992). Development of a repair-enrichment broth for resuscitation of heat-injured Listeria monocytogenes and Listeria innocua. *Appl. Environ. Microbiol.* 58 (1), 14–20. doi:10.1128/AEM.58.1.14-20.1992

Chignell, C. F., Bilskj, P., Reszka, K. J., Motten, A. G., Sik, R. H., and Dahl, T. A. (1994). Spectral and photochemical properties of curcumin. *Photochem. Photobiol.* 59 (3), 295–302. doi:10.1111/j.1751-1097.1994.tb05037.x

Colaruotolo, L. A., Peters, E., and Corradini, M. G. (2021). Novel luminescent techniques in aid of food quality, product development, and food processing. *Curr. Opin. Food Sci.* 42, 148–156. doi:10.1016/j.cofs.2021.06.005

Corradini, M., and Peleg, M. (2005). Estimating non-isothermal bacterial growth in foods from isothermal experimental data. *J. Appl. Microbiol.* 99 (1), 187–200. doi:10.1111/j.1365-2672.2005.02570.x

Cossu, M., Ledda, L., and Cossu, A. (2021). Emerging trends in the photodynamic inactivation (PDI) applied to the food decontamination. *Food Res. Int.* 144, 110358. doi:10.1016/j.foodres.2021.110358

Dahl, T. A., McGowan, W. M., Shand, M. A., and Srinivasan, V. S. (1989). Photokilling of bacteria by the natural dye curcumin. *Archives Microbiol.* 151 (2), 183–185. doi:10.1007/BF00414437

De La Maza, A., Parra, J., Garcia, M., Ribosa, I., and Leal, J. S. (1992). Permeability changes in the phospholipid bilayer caused by nonionic surfactants. *J. colloid interface Sci.* 148 (2), 310–316. doi:10.1016/0021-9797(92)90170-q

Demidova, T. N., and Hamblin, M. R. (2005). Effect of cell-photosensitizer binding and cell density on microbial photoinactivation. *Antimicrob. agents Chemother.* 49 (6), 2329–2335. doi:10.1128/AAC.49.6.2329-2335.2005

de Oliveira, E. F., Tosati, J. V., Tikekar, R. V., Monteiro, A. R., and Nitin, N. (2018). Antimicrobial activity of curcumin in combination with light against *Escherichia coli* O157: H7 and Listeria innocua: applications for fresh produce sanitation. *Postharvest Biol. Technol.* 137, 86–94. doi:10.1016/j.postharvbio.2017.11.014

Duan, Y., Wang, J., Yang, X., Du, H., Xi, Y., and Zhai, G. (2015). Curcumin-loaded mixed micelles: preparation, optimization, physicochemical properties and cytotoxicity *in vitro*. *Drug Deliv.* 22 (1), 50–57. doi:10.3109/10717544.2013.873501

Dysart, J. S., and Patterson, M. S. (2005). Characterization of Photofrin photobleaching for singlet oxygen dose estimation during photodynamic therapy of MLL cells *in vitro*. *Phys. Med. Biol.* 50 (11), 2597–2616. doi:10.1088/0031-9155/50/11/011

Espina, L., García-Gonzalo, D., and Pagán, R. (2016). Detection of thermal sublethal injury in *Escherichia coli* via the selective medium plating technique: mechanisms and improvements. *Front. Microbiol.* 7, 1376. doi:10.3389/fmicb.2016.01376

Gaysinsky, S. (2004). Physicochemical and antimicrobial properties of antimicrobials encapsulated in surfactant-based nanoparticles (Masters). Knoxville: University of Tennesse. Available at: https://trace.tennessee.edu/utk_gradthes/2193.

Gaysinsky, S., Davidson, P. M., Bruce, B. D., and Weiss, J. (2005). Stability and antimicrobial efficiency of eugenol encapsulated in surfactant micelles as affected by temperature and pH. *J. food Prot.* 68 (7), 1359–1366. doi:10.4315/0362-028x-68.7.1359

Gu, G., Ottesen, A., Bolten, S., Luo, Y., Rideout, S., and Nou, X. (2020). Microbiome convergence following sanitizer treatment and identification of sanitizer resistant species from spinach and lettuce rinse water. *Int. J. food Microbiol.* 318, 108458. doi:10.1016/j.ijfoodmicro.2019.108458

Hammer, K., Carson, C., and Riley, T. (1999). Influence of organic matter, cations and surfactants on the antimicrobial activity of Melaleuca alternifolia (tea tree) oil *in vitro*. *J. Appl. Microbiol.* 86 (3), 446–452. doi:10.1046/j.1365-2672.1999.00684.x

Inouye, S., Tsuruoka, T., Uchida, K., and Yamaguchi, H. (2001). Effect of sealing and Tween 80 on the antifungal susceptibility testing of essential oils. *Microbiol. Immunol.* 45 (3), 201–208. doi:10.1111/j.1348-0421.2001.tb02608.x

Jameson, D. M. (2014). *Introduction to fluorescence*. Boca Raton: CRC Press.

Karaffa, L. S. (2013). *The Merck index: an encyclopedia of chemicals, drugs, and biologicals*. USA: RSC Publishing.

Kharat, M., Du, Z., Zhang, G., and McClements, D. J. (2017). Physical and chemical stability of curcumin in aqueous solutions and emulsions: impact of pH, temperature, and molecular environment. *J. Agric. food Chem.* 65 (8), 1525–1532. doi:10.1021/acs.jafc.6b04815

Komaiko, J. S., and McClements, D. J. (2016). Formation of food-grade nanoemulsions using low-energy preparation methods: a review of available methods. *Compr. Rev. food Sci. food Saf.* 15 (2), 331–352. doi:10.1111/1541-4337.12189

Langsrud, S., Sundheim, G., and Borgmann-Strahsen, R. (2003). Intrinsic and acquired resistance to quaternary ammonium compounds in food-related Pseudomonas spp. *J. Appl. Microbiol.* 95 (4), 874–882. doi:10.1046/j.1365-2672.2003.02064.x

Lauro, F. M., Pretto, P., Covolo, L., Jori, G., and Bertoloni, G. (2002). Photoinactivation of bacterial strains involved in periodontal diseases sensitized by porphycene–polylysine conjugates. *Photochem. Photobiological Sci.* 1 (7), 468–470. doi:10.1039/b200977c

Macdonald, I. J., and Dougherty, T. J. (2001). Basic principles of photodynamic therapy. *J. Porphyr. Phthalocyanines* 5 (02), 105–129. doi:10.1002/jpp.328

Maisch, T., Szeimies, R.-M., Jori, G., and Abels, C. (2004). Antibacterial photodynamic therapy in dermatology. *Photochem. Photobiological Sci.* 3 (10), 907–917. doi:10.1039/b407622b

McLaughlin, H. P., and Sue, D. (2018). Rapid antimicrobial susceptibility testing and β-lactam-induced cell morphology changes of Gram-negative biological threat pathogens by optical screening. *BMC Microbiol.* 18 (1), 218–315. doi:10.1186/s12866-018-1347-9

Romanova, N., Wolffs, P., Brovko, L., and Griffiths, M. (2006). Role of efflux pumps in adaptation and resistance of Listeria monocytogenes to benzalkonium chloride. *Appl. Environ. Microbiol.* 72 (5), 3498–3503. doi:10.1128/AEM.72.5.3498-3503.2006

Ryu, V., McClements, D. J., Corradini, M. G., Yang, J. S., and McLandsborough, L. (2018). Natural antimicrobial delivery systems: formulation, antimicrobial activity, and mechanism of action of quillaja saponin-stabilized carvacrol nanoemulsions. *Food Hydrocoll.* 82, 442–450. doi:10.1016/j.foodhyd.2018.04.017

Ryu, V., Ruiz-Ramirez, S., Chuesiang, P., McLandsborough, L. A., McClements, D. J., and Corradini, M. G. (2021). Use of micellar delivery systems to enhance curcumin's stability and microbial photoinactivation capacity. *Foods* 10 (8), 1777. doi:10.3390/foods10081777

Schweitzer, C., and Schmidt, R. (2003). Physical mechanisms of generation and deactivation of singlet oxygen. *Chem. Rev.* 103 (5), 1685–1757. doi:10.1021/cr010371d

Sharma, V., Borse, M., Devi, S., Dave, K., Pohnerkar, J., and Prajapati, A. (2005). Oil solubilization capacity, liquid crystalline properties, and antibacterial activity of alkanolamine-based novel cationic surfactants. *J. dispersion Sci. Technol.* 26 (4), 421–427. doi:10.1081/dis-200054563

Tønnesen, H. H., and Karlsen, J. (1985). Studies on curcumin and curcuminoids. VI. Kinetics of curcumin degradation in aqueous solution. *Z. für Lebensm. Forsch.* 180 (5), 402–404. doi:10.1007/BF01027775

Tsai, T., Yang, Y. T., Wang, T. H., Chien, H. F., and Chen, C. T. (2009). Improved photodynamic inactivation of gram-positive bacteria using hematoporphyrin encapsulated in liposomes and micelles. *Lasers Surg. Med. Official J. Am. Soc. Laser Med. Surg.* 41 (4), 316–322. doi:10.1002/lsm.20754

Turro, N. J., Ramamurthy, V., and Scaiano, J. C. (2017). *Modern molecular photochemistry of organic molecules*. Sausalito: Viva Books University Science Books.

Yang, X., Rai, R., Huu, C. N., and Nitin, N. (2019). Synergistic antimicrobial activity by light or thermal treatment and lauric arginate: membrane damage and oxidative stress. *Appl. Environ. Microbiol.* 85 (17), e01033-19–e01019. doi:10.1128/AEM.01033-19

Zorofchian Moghadamtousi, S., Abdul Kadir, H., Hassandarvish, P., Tajik, H., Abubakar, S., and Zandi, K. (2014). A review on antibacterial, antiviral, and antifungal activity of curcumin. *BioMed Res. Int.* 2014, 186864. doi:10.1155/2014/186864